



Chemistry and structure by design: ordered CuNi(CN)₄ sheets with copper(II) in a square-planar environment

Article

Accepted Version

Chippindale, A. M., Hibble, S. J., Marelli, E., Bilbe, E. J., Hannon, A. C. and Zbiri, M. (2015) Chemistry and structure by design: ordered CuNi(CN)₄ sheets with copper(II) in a square-planar environment. Dalton Transactions, 44 (28). pp. 12502-12506. ISSN 1364-5447 doi: <https://doi.org/10.1039/c5dt01127b> Available at <http://centaur.reading.ac.uk/40776/>

It is advisable to refer to the publisher's version if you intend to cite from the work.

To link to this article DOI: <http://dx.doi.org/10.1039/c5dt01127b>

Publisher: Royal Society of Chemistry

All outputs in CentAUR are protected by Intellectual Property Rights law, including copyright law. Copyright and IPR is retained by the creators or other copyright holders. Terms and conditions for use of this material are defined in the [End User Agreement](#).

www.reading.ac.uk/centaur

CentAUR

Central Archive at the University of Reading

Reading's research outputs online

COMMUNICATION

**Chemistry and Structure by Design: Ordered
CuNi(CN)₄ Sheets with Copper(II) in a Square-Planar
Environment**

Cite this: DOI: 10.1039/x0xx00000x

Received 00th January 2012,
Accepted 00th January 2012

DOI: 10.1039/x0xx00000x

www.rsc.org/A. M. Chippindale,^{*a} S. J. Hibble,^{*b} E. Marelli,^a E. J. Bilbe,^a A. C. Hannon^c and M. Zbiri^d

COMMUNICATION

Layered copper-nickel cyanide, $\text{CuNi}(\text{CN})_4$, a 2-D negative thermal expansion material, is one of a series of copper(II)-containing cyanides derived from $\text{Ni}(\text{CN})_2$. In $\text{CuNi}(\text{CN})_4$, unlike in $\text{Ni}(\text{CN})_2$, the cyanide groups are ordered generating square-planar $\text{Ni}(\text{CN})_4$ and $\text{Cu}(\text{NC})_4$ units. The adoption of square-planar geometry by $\text{Cu}(\text{II})$ in an extended solid is very unusual.

The simple binary copper(II) cyanide, $\text{Cu}(\text{CN})_2$, does not exist. The reaction of $\text{Cu}(\text{II})$ in aqueous solution with the pseudohalide cyanide ion reacts via a number of steps to produce cyanogen and copper(I) cyanide, CuCN .¹ This is reminiscent of the reaction familiar to chemistry undergraduates in which the iodide ion reacts with copper(II) to produce iodine and copper(I) iodide.²



Our challenge was to stabilize $\text{Cu}(\text{II})$ with respect to the internal redox reaction in the presence of cyanide ligands only. This has been achieved by replacement of half of the $\text{Ni}(\text{II})$ in anhydrous nickel cyanide, $\text{Ni}(\text{CN})_2$, by $\text{Cu}(\text{II})$ to form $\text{CuNi}(\text{CN})_4$. In $\text{Ni}(\text{CN})_2$, each Ni atom is linked by four linear, bridging cyanide ions to four other nickel atoms to form planar $\text{Ni}(\text{CN})_2$ sheets with head-to-tail cyanide disorder.³⁻⁵ By using the square-planar ion, $[\text{Ni}(\text{CN})_4]^{2-}$, as a synthon and linking such units by Cu^{2+} ions, a modified $\text{Ni}(\text{CN})_2$ sheet structure can be assembled in which the copper atoms have square-planar geometry and are coordinated only to cyanide ligands *via* nitrogen to generate an ordered sheet (Figure 1).[#]

Although there are a number of examples of molecular species containing square-planar $\text{Cu}(\text{II})$ with, for example, phthalocyanines and N and O donor ligands,^{7,8} we believe that the layered product, $\text{CuNi}(\text{CN})_4$, is the first example of a simple extended solid containing Cu^{2+} (d^9) ions in X-ray diffraction patterns of $\text{CuNi}(\text{CN})_4$ at 30, 180 and 270 °C (303, 453 and 543 K) square-planar coordination. The separation between adjacent $\text{CuNi}(\text{CN})_4$ layers at 3.09 Å is too great for significant interlayer interactions to occur, precluding Jahn-Teller distortion of octahedral geometry to produce (4+2) coordination, as is frequently observed in Cu^{2+} compounds. Further exploration of the $\text{Cu}(\text{II})$ - $\text{Ni}(\text{II})$ cyanide phase diagram shows that $\text{Cu}(\text{II})$ containing compounds also exist both as hydrates, $\text{Cu}_x\text{Ni}_{1-x}(\text{CN})_2 \cdot 3\text{H}_2\text{O}$, and dehydrated phases, $\text{Cu}_x\text{Ni}_{1-x}(\text{CN})_2$, forming solid solutions over the range ($0 \leq x \leq 0.25$).

The addition of Cu^{2+} ions to $\text{Ni}(\text{CN})_4^{2-}$ in aqueous solution immediately produces a blue-green gelatinous precipitate (*vide infra*), which on stirring for several hours transforms to a grey solid, characterised as $\text{CuNi}(\text{CN})_4$. On heating $\text{CuNi}(\text{CN})_4$ under nitrogen at 680 K, copper(II) is reduced by cyanide to produce copper(I) cyanide and paracyanogen, together with nickel cyanide, according to the reaction:



Figure 2 shows the powder X-ray diffraction patterns obtained for $\text{CuNi}(\text{CN})_4$ and $\text{Ni}(\text{CN})_2$. The Bragg peak positions and relative intensities show the close underlying similarity of the two structures and confirm that $\text{CuNi}(\text{CN})_4$ is a layered material. The difference in peak widths in the two diffraction patterns arises mainly from the difference in crystallite size of the two materials. The Raman spectrum of $\text{CuNi}(\text{CN})_4$ exhibits 2 $\nu_{\text{C}\equiv\text{N}}$ stretches, at 2209 and 2184 cm^{-1} , and the infrared spectrum has one non-coincident $\nu_{\text{C}\equiv\text{N}}$ stretch

at 2182 cm^{-1} . These observations are consistent with D_{4h} symmetry of the individual metal-cyanide layers. Only two arrangements of the

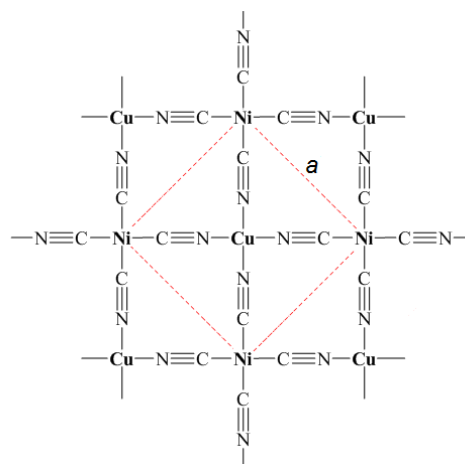


Fig. 1 Representation of a layer of $\text{CuNi}(\text{CN})_4$ with square-planar geometry around both Cu^{2+} and Ni^{2+} ions. The structural repeat unit within the layer is shown in the red square of length a .

metal atoms and cyanide groups within each layer are therefore possible: namely, the one shown in Figure 1, with the carbon end of the cyanide ligand attached to nickel and the nitrogen end to copper, or the inverted arrangement with the carbon end attached to copper. Of these two possibilities, only the first arrangement yields a good fit to the low r region ($0 < r/\text{Å} < 3$) of the total correlation function, $T^N(r)_{\text{exp}}$, obtained from neutron diffraction (Figure 3 and S.10) confirming that the metals and cyanide groups in $\text{CuNi}(\text{CN})_4$ are indeed arranged as shown in Figure 1. The bond lengths obtained from the fitting of individual peaks in $T^N(r)_{\text{exp}}$ at 15 K are: $\text{C}\equiv\text{N}$, 1.1541(6); $\text{Ni}-\text{C}$, 1.857(1) and $\text{Cu}-\text{N}$, 1.943(2) Å.

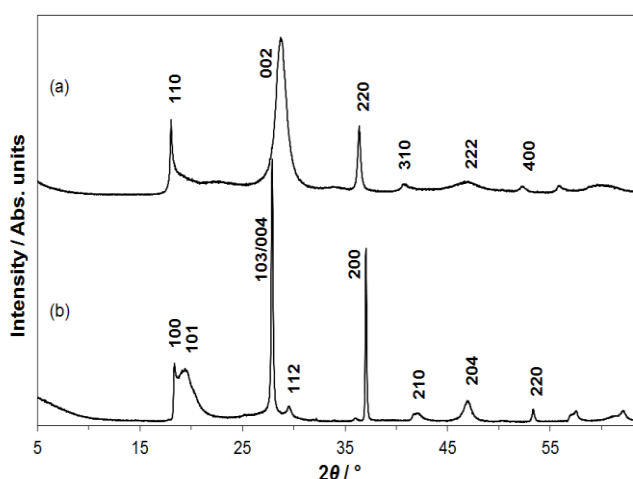


Fig. 2 Powder X-ray diffraction patterns at 295 K of (a) $\text{CuNi}(\text{CN})_4$ ($a = 6.957(1)$ and $c = 6.180(6)$ Å) and (b) $\text{Ni}(\text{CN})_2$ ($a = 4.857$ and $c = 12.802$ Å)³ ($\text{Cu } K\alpha_1$ radiation, $\lambda = 1.54060$ Å) showing Miller indices of the principal reflections.

Taking into account the metal and cyanide ordering within the layers determined above, the powder X-ray diffraction pattern for

$\text{CuNi}(\text{CN})_4$ can be indexed on a tetragonal unit cell ($a = 6.957(1)$ and $c = 6.180(6)$ Å) (Figure 2). This unit cell is related to that of $\text{Ni}(\text{CN})_2$. The a lattice parameter in $\text{CuNi}(\text{CN})_4$ is $\sim\sqrt{2}$ of the value for $\text{Ni}(\text{CN})_2$ as a consequence of the ordering of the Cu and Ni atoms within the layers. X-ray and neutron diffraction experiments³ show no evidence of cyanide ordering within the nickel-cyanide layers in $\text{Ni}(\text{CN})_2$ and in this case, the a lattice parameter corresponds to the direct M–CN–M distance shown in Figure 1. The c lattice parameter chosen for $\text{CuNi}(\text{CN})_4$ corresponds to a two-layer repeat, *ABAB*, and a physically reasonable interlayer separation of ~ 3.09 Å. Although a c lattice parameter of 1/2 this value could be used to index fully the powder X-ray pattern of $\text{CuNi}(\text{CN})_4$, this would be physically unreasonable as in the resulting *AAA* stacking, the atoms in adjacent layers would lie directly above each other and hence be impossibly close together. The stacking sequence in $\text{Ni}(\text{CN})_2$ is more complicated with a four-layer repeat predominating^{3,4} resulting in a c lattice parameter of ~ 12.8 Å and the appearance of the broad reflection, indexed as (101), seen at $2\theta \sim 20^\circ$ (Figure 2(b)).

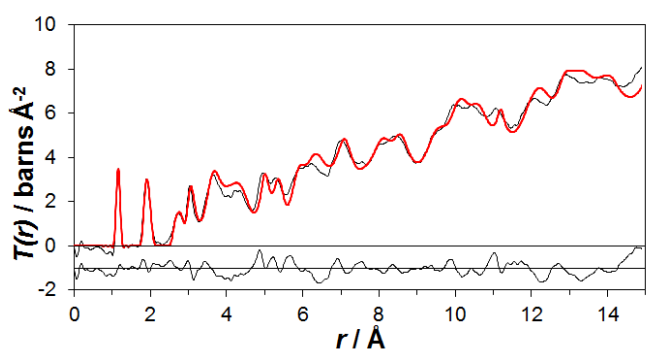


Fig. 3 Total correlation functions for $\text{CuNi}(\text{CN})_4$ at 15 K: $T^N(r)_{\text{exp}}$ (black line) and, for a model in *Cmcm*, $T^N(r)_{\text{mod}}$ (red line). The difference function is shown at the bottom of the plot (offset for clarity by 1 barns Å⁻²).

Using the Cu–N, Ni–C and C≡N bond lengths obtained from fitting the low r region of $T^N(r)_{\text{exp}}$ (Figure 3), together with the unit-cell parameters obtained from the powder X-ray diffraction pattern and including the *ABAB* stacking of the layers, a 3-D model was constructed in space group *Cmcm* (Figure 4). This model reproduces $T^N(r)_{\text{exp}}$ to $r = 15$ Å well (Figure 3) and is thus a good representation of the short- and medium-range structure in the material.[‡] It should be noted that this conventional crystallographic model does not fully reproduce the powder X-ray diffraction pattern in Figure 2 because in $\text{CuNi}(\text{CN})_4$, there is extensive stacking disorder, as evidenced by the shape of the (110) reflection (Figure 2). Hence although the model gives a good description of the short- and medium-range order in $\text{CuNi}(\text{CN})_4$, the chemically important information, it needs to be combined with a model of the stacking disorder in order to reproduce the powder X-ray pattern. Indeed, an appropriate calculation demonstrating this has already been carried out in a previous paper⁴ in which different types of stacking disorder were considered for $\text{Ni}(\text{CN})_2$ and has validity in the present case as the X-ray scattering factors of Cu and Ni are very similar (as indeed are those of C and N). The simulated powder X-ray diffraction pattern in which the sequence *AB* is followed by *A* occurs with a probability of 75% gives a good match to our observed pattern. In contrast, in $\text{Ni}(\text{CN})_2$, the most probable stacking sequence (67%) is that the sequence *AB* is followed by a third layer, *A'*, which is offset with respect to both *A* and *B*.

Layered inorganic materials are currently attracting much interest, particularly with respect to their electronic, optical and mechanical properties.⁹ Although graphene and metal disulfides are the most widely studied, a recent paper utilising DFT calculations has suggested that $\text{Ni}(\text{CN})_2$ should have interesting electronic properties

when in the form of individual sheets and, by analogy with graphene, when rolled into nanotubes, particularly if it can be n or p doped.¹⁰ Mo and Kaxiras proposed that doping could be achieved by replacing some of the $-\text{C}\equiv\text{N}-$ linkages by $-\text{C}\equiv\text{C}-$ or $-\text{N}=\text{N}-$ groups to produce either p - or n -doped structures. In our synthesis of $\text{CuNi}(\text{CN})_4$, we have effectively substituted on the metal sites in $\text{Ni}(\text{CN})_2$, rather than the non-metal sites. By replacing half the Ni^{2+} by Cu^{2+} in $\text{Ni}(\text{CN})_2$ to form $\text{CuNi}(\text{CN})_4$, we have achieved an extremely high level of n doping of the layers. The magnetic susceptibility of $\text{CuNi}(\text{CN})_4$ has the value $\mu = 1.76 \mu_B$ at 295 K, which is consistent with isolated moments on Cu^{2+} ions (d^9), and unfortunately indicates that a delocalised electron system is not formed. The presence of an absorption band centred at ~ 17000 cm⁻¹ in the diffuse reflectance spectrum of $\text{CuNi}(\text{CN})_4$ can be ascribed to a d - d transition(s) and is unobserved in the corresponding spectrum of $\text{Ni}(\text{CN})_2$ (Figure 5). From the reflectance spectra, the optical band gaps for $\text{Ni}(\text{CN})_2$ and $\text{CuNi}(\text{CN})_4$ are determined to be 16100 and 21780 cm⁻¹ (2 and 2.7 eV), respectively, showing that this degree of substitution of Ni by Cu has produced a poorer semiconductor as a result of ordering within the metal-cyanide sheets.

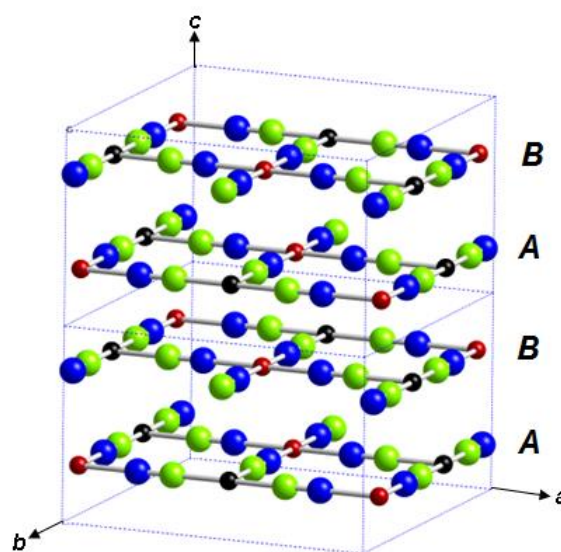


Fig. 4 Model of $\text{CuNi}(\text{CN})_4$ in space group *Cmcm* ($a = b = 9.9082$ and $c = 6.100$ Å) showing the *ABAB* stacking of the ordered layers. (Key: copper atoms, orange spheres; nickel atoms, black spheres; carbon atoms, green spheres and nitrogen atoms, blue spheres).

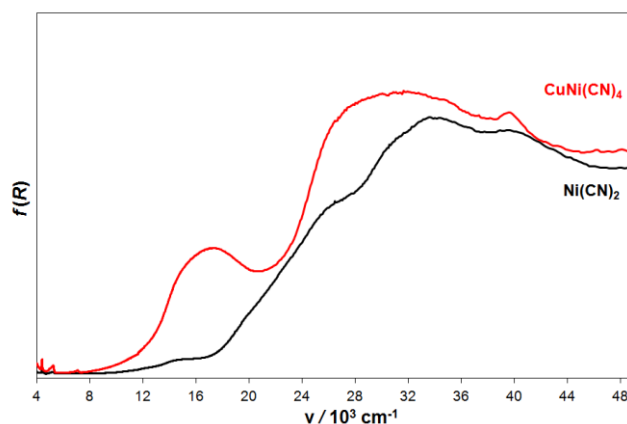


Fig. 5 Diffuse reflectance spectra of $\text{CuNi}(\text{CN})_4$ (red) and $\text{Ni}(\text{CN})_2$ (black)

Considering mechanical properties, $\text{CuNi}(\text{CN})_4$ shows two-dimensional negative thermal expansion with $\alpha_a = -9.7(8) \times 10^{-6} \text{ K}^{-1}$ (where $\alpha_a = (a_{T_2} - a_{T_1})/a_{T_1}(T_2 - T_1)$) (Figure 6) which is of a similar magnitude to that measured for graphene¹¹ and ~ 1.5 times the value for $\text{Ni}(\text{CN})_2$. Inelastic neutron scattering and DFT studies on $\text{Ni}(\text{CN})_2$ at ambient⁵ and high pressure¹² show that it is the atomic motions perpendicular to the metal-cyanide sheets that give rise to the 2-D NTE behaviour and it is anticipated that similar mechanism will apply in the case of $\text{CuNi}(\text{CN})_4$. Figure 6 shows the relative percentage changes in the a and c lattice parameters and cell volume, V , for $\text{CuNi}(\text{CN})_4$ and $\text{Ni}(\text{CN})_2$. Although α_a is independent of temperature over the temperature range of this study for both $\text{CuNi}(\text{CN})_4$ and $\text{Ni}(\text{CN})_2$, the temperature dependence of α_c is different for the two materials. For $\text{CuNi}(\text{CN})_4$, α_c is non linear with temperature, whereas for $\text{Ni}(\text{CN})_2$, it is, like α_a , independent of temperature. An explanation of the difference in the form of the variation of the c parameter with temperature, and hence also cell volume, requires a detailed comparison of the phonon density of states of $\text{CuNi}(\text{CN})_4$ and $\text{Ni}(\text{CN})_2$ to be carried out over a comparable temperature range.

As well as being mechanically different from $\text{Ni}(\text{CN})_2$, copper nickel cyanide, $\text{CuNi}(\text{CN})_4$, is chemically different in that it does not form hydrates. Indeed, it can be obtained directly from aqueous solution as the anhydrous compound, as described above. (Similar reactions using only nickel reagents, *e.g.* $\text{Ni}^{2+} + \text{Ni}(\text{CN})_4^{2-}$, produce layered nickel-cyanide hydrates, $\text{Ni}(\text{CN})_2 \cdot n\text{H}_2\text{O}$ ($n = 3, 3/2$), containing $\text{Ni}(\text{CN})_4(\text{H}_2\text{O})_2$ and $\text{Ni}(\text{CN})_4$ units, and dehydration is required to form $\text{Ni}(\text{CN})_2$.³

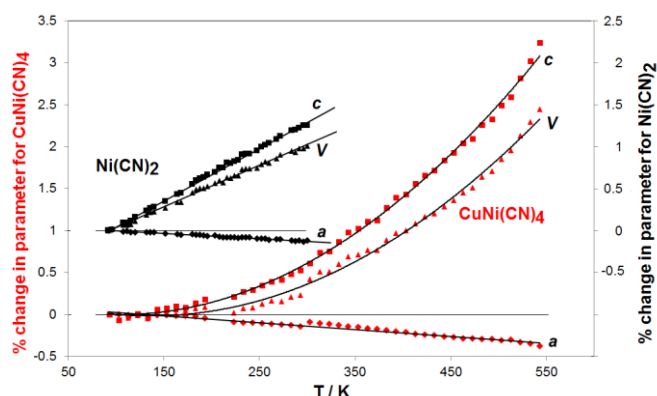


Fig. 6 The relative percentage changes in the a and c lattice parameters and volume, V , for $\text{CuNi}(\text{CN})_4$ and $\text{Ni}(\text{CN})_2$ ³ over the temperature ranges (93 - 543) K and (95 - 295) K, respectively. The relative % change of a parameter, l_{T_2} , is given by $100 \times (l_{T_2} - l_{T_1})/l_{T_1}$, where l_{T_2} is the parameter l at temperature T_2 , and l_{T_1} is the parameter l at the lowest temperature, T_1 .

$\text{CuNi}(\text{CN})_4$ is probably initially formed as individual layers. Mixing the salt solutions produces at first a blue gel, which turns grey on ageing in solution or on drying as the individual layers aggregate to form stacks. The powder X-ray diffraction patterns shown in Figure 7 provide evidence that the material grows only slowly in the [001] direction. Even in its final grey form, the stacks in $\text{CuNi}(\text{CN})_4$ are only $\sim 40 \text{ \AA}$ thick (as estimated by using the Scherrer equation applied to the (002) reflection). The slow growth in the c direction occurs possibly because the bonding between the layers is weak. Support for this hypothesis comes from the ease of separating the layers to make intercalation compounds. For example, stirring $\text{CuNi}(\text{CN})_4$ in 4,4'-bipyridine in ethanol at room temperature produces a blue-grey solid with an interlayer separation of $\sim 11.3 \text{ \AA}$, consistent with the formation of a pillared-layer compound, $\text{CuNi}(\text{CN})_4(\text{bipy})_x$, which is distinct from the previously reported material, $\text{CuNi}(\text{CN})_4[\text{bipy}](\text{H}_2\text{O})_2$,¹³ in which $-\text{Cu}(\text{OH})_2-\text{NC}-\text{Ni}(\text{CN})_2-\text{CN}-$ zig-zag chains are linked through 4,4'-bipyridine groups.

Further exploration of the $\text{Cu}(\text{CN})_2$ - $\text{Ni}(\text{CN})_2$ phase diagram required a different method of synthesis in which Cu^{2+} and Ni^{2+} were simultaneously added to a cyanide solution. Using this method at more nickel-rich compositions than $\text{CuNi}(\text{CN})_4$ ($(\text{Cu}_{1/2}\text{Ni}_{1/2}(\text{CN})_2)$), mixtures of $\text{CuNi}(\text{CN})_4$ and the hydrate $\text{Cu}_{1/4}\text{Ni}_{3/4}(\text{CN})_2 \cdot 3\text{H}_2\text{O}$ were produced. At even higher nickel contents, a solid-solution region, $\text{Cu}_x\text{Ni}_{1-x}(\text{CN})_2 \cdot 3\text{H}_2\text{O}$ ($0 \leq x \leq 0.25$), formed. The hydrates can be easily dehydrated to form the $\text{Cu}_x\text{Ni}_{1-x}(\text{CN})_2$ phases shown in Figure 8, which all adopt a nickel-cyanide-type structure. No mixed Cu(II)-

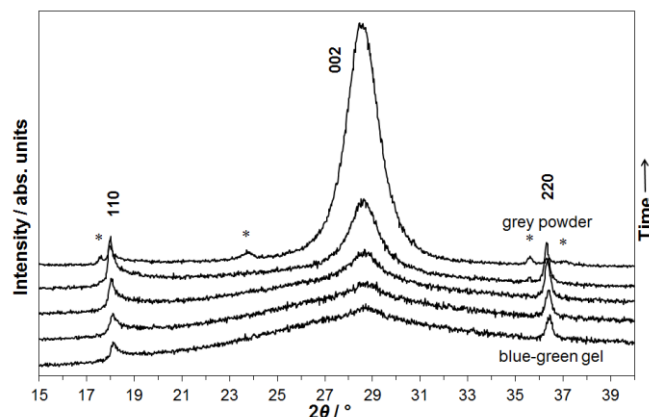


Fig. 7 *In situ* powder XRD patterns collected during the drying of $\text{CuNi}(\text{CN})_4$ as the sample turned from a blue-green gelatinous solid to a grey powder. The (002) reflection at $\sim 29^\circ$ increases in intensity on drying, whilst the (110) and (220) reflections remain substantially unchanged as the number of already-formed 2-D layers stacking together increases.

$\text{Ni}(\text{II})$ cyanides containing more copper than nickel could be prepared and the additional copper Cu(II) is reduced to Cu(I) in the form of the low-temperature polymorph of copper (I) cyanide, LT-CuCN.¹⁴ This reduction was also found when preparing the mixed Cu(I)-Cu(II) phase, $\text{Cu}_2\text{Ni}(\text{CN})_5 \cdot 3\text{H}_2\text{O}$, from Cu(II) and $\text{Ni}(\text{CN})_4^{2-}$.¹⁵ In copper rich compounds, $\text{Cu}_x\text{Ni}_{1-x}(\text{CN})_2$ ($x > 0.5$), some Cu(II) atoms would have to be coordinated to the carbon end of cyanide groups and it might be this fact that leads to their instability. Although rare, it should be noted that Cu(II) can be attached to cyanide groups *via* the carbon end of the ligand, for example, in $[\text{Cu}(\text{phen})_2\text{CN}]^+$,¹⁶ and of particular note is the molecular compound, $\text{Cu}(\text{phen})(\text{CN})_2$, which has Cu(II) connected to two CN groups in this way.¹⁷

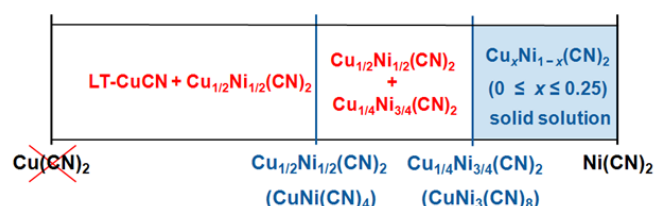


Fig. 8 Phases formed in the Cu(II)-Ni(II)-cyanide system.

In conclusion, we have prepared a number of new layered compounds, $\text{Cu}_x\text{Ni}_{1-x}(\text{CN})_2$, consisting of $\text{M}(\text{CN})_2$ sheets structurally related to those found in $\text{Ni}(\text{CN})_2$. Addition of the synthon, $[\text{Ni}(\text{CN})_4]^{2-}$, to Cu^{2+} in aqueous solution, leads to the precipitation of anhydrous $\text{CuNi}(\text{CN})_4$. A combination of powder X-ray and total neutron diffraction, together with vibrational spectroscopy, has established that in $\text{CuNi}(\text{CN})_4$ ($(\text{Cu}_{1/2}\text{Ni}_{1/2}(\text{CN})_2)$), the cyanide ligands bind so that their carbon atoms are coordinated only to nickel

and their nitrogen atoms only to copper to generate ordered sheets containing square-planar Ni(CN)₄ and Cu(CN)₄ units. The stabilising of Cu^{II} in an environment with cyanide as the only ligand present has not previously been reported. CuNi(CN)₄ shows two-dimensional negative thermal expansion. We are currently analysing the phonon density of states of CuNi(CN)₄ to discover why it shows very different thermal expansion behaviour from Ni(CN)₂ perpendicular to the metal-cyanide layers.

In contrast to CuNi(CN)₄, which can be prepared directly as an anhydrous compound from aqueous solution, other, more nickel-rich Cu_xNi_{1-x}(CN)₂ compounds are formed *via* the hydrates, Cu_xNi_{1-x}(CN)₂·3H₂O, which can be easily dehydrated. A solubility gap exists between CuNi(CN)₄, the most copper-rich phase that can be formed and a region of solid solution which exists between Cu_{1/4}Ni_{3/4}(CN)₂ and Ni(CN)₂.

The authors thank the EPSRC (EP/G067279/1) and STFC (CMPC06101) for studentships for EM and EJB, respectively. The University of Reading is acknowledged for provision of the Chemical Analysis Facility (CAF).

Notes and references

^a Department of Chemistry, University of Reading, Whiteknights, Reading RG6 6AD, UK. E mail: a.m.chippindale@rdg.ac.uk; Fax: +44 (0)1183786331; Tel: +44 (0)118 3788448

^b present address: Jesus College, Oxford OX1 3DW, UK.

^c ISIS Facility, Rutherford Appleton Laboratory, Chilton, Didcot, OX11 0QX, UK

^d Institut Laue-Langevin, BP 156, F-38042 Grenoble Cedex 9, France

[#]FOOTNOTE: Although ordering of cyanide groups often occurs in mixed-metal cyanides, this is not always the case. For example, in the series of mixed-metal cyanides containing Cu(I), (Cu_{1/2}Au_{1/2})CN contains ordered chains of the type [Au–C≡N–Cu–N≡C–]_n, whereas in (Cu_{1/2}Ag_{1/2})CN, there is head-to-tail cyanide disorder.⁶

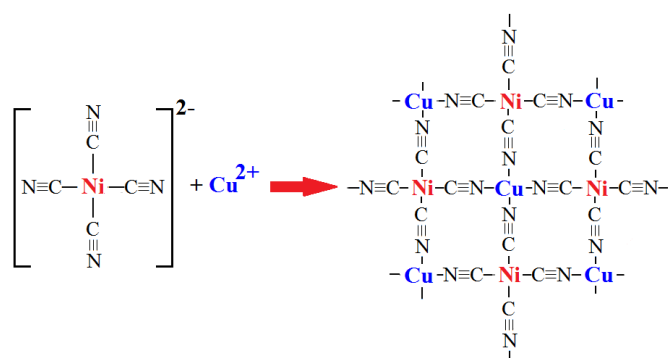
[‡]FOOTNOTE: Although stacking together layers of *D*_{4h} symmetry in an *ABAB* sequence is incompatible with true tetragonal symmetry, it is possible to construct orthorhombic models with a tetragonal metric. Furthermore, stacking disorder will lead to the long-range average metric appearing tetragonal, so that a model describing the local and intermediate structure in *Cmcm* is not in conflict with the indexing of the powder X-ray pattern as tetragonal.

† Electronic Supplementary Information (ESI) available: Synthesis of CuNi(CN)₄ and Cu_xNi_{1-x}(CN)₂ phases; X-ray powder diffraction patterns (variable temperature); neutron powder total diffraction details; thermal analysis; IR and Raman spectroscopy data, magnetic data. See DOI: 10.1039/c000000x/

- 1 A. G. Sharpe in 'The Chemistry of Cyano Complexes of the Transition Metals', Academic Press Inc London, 1976.
- 2 C. E. Housecroft and A. G. Sharpe, *Inorganic Chemistry*, Pearson Education Ltd, UK, 4th Edn, p 768.
- 3 S. J. Hibble, A. M. Chippindale, A. H. Pohl and A. C. Hannon, *Angew. Chem. Int. Ed.*, 2007, **46**, 7116.
- 4 A. L. Goodwin, M. T. Dove, A. M. Chippindale, S. J. Hibble, A. H. Pohl and A. C. Hannon, *Phys. Rev B: Condens. Matter.*, 2009, **B80**, 054101.

- 5 R. Mittal, M. Zbiri, H. Schober, E. Marelli, S. J. Hibble, A. M. Chippindale and S. L. Chaplot, *Phys. Rev B: Condens. Matter.*, 2011, **B83**, 024301.
- 6 A. M. Chippindale, S. J. Hibble, E. J. Bilbé, E. Marelli, A. C. Hannon, C. Allain, R. Pansu, and F. Hartl, *J. Am. Chem. Soc.*, 2012, **134**, 16387.
- 7 C. J. Brown, *J. Chem. Soc. A*, 1968, 2488.
- 8 M. Melnik, M. Kabesova, M. Dunaj-Jurco and C. E. Holloway, *J. Coord. Chem.*, 1997, **41**, 35.
- 9 Q. H. Wang, K. Kalantar-Zadeh, A. Kis, J. N. Coleman and M. S. Strano, *Nature Nanotechnol.*, 2012, **7**, 699.
- 10 Y. Mo and E. Kaxiras, *Small*, 2007, **3**, 1253.
- 11 D. Yoon, Y. W. Son and H. Cheong *Nano Lett.*, 2011, **11**, 3227.
- 12 S. K. Mishra, R. Mittal, M. Zbiri, R. Rao, P. Goel, S. J. Hibble, A. M. Chippindale, T. Hansen, H. Schober and S. L. Chaplot, arXiv:1409.2305 [cond-mat.mtrl-sci].
- 13 O. Sereda and H. Stoeckli-Evans, *Acta Cryst.*, 2008, **C64**, m221.
- 14 S. J. Hibble, S. G. Eversfield, A. R. Cowley and A. M. Chippindale, *Angew. Chem. Int. Ed.* **2004**, **43**, 628.
- 15 Y. L. Qin, R. X. Yao, G. X. Wu, M. M. Liu, and X. M. Zhang, *Chem. Asian J.*, 2013, **8**, 1587.
- 16 M. Dunaj-Jurco, I. Potocnak, J. Cibik and M. Kabesova, V. Kettmann And D Miklos, *Acta Cryst.* 1993, **C49**, 1479.
- 17 M. Wicholas and T. Wolford, *Inorg. Chem.*, 1974, **13**, 316.

Graphical Abstract



Cu(II) has been stabilised with square-planar coordination in a cyanide-only environment in the layered semiconducting material, copper-nickel cyanide, CuNi(CN)₄, which shows 2-D negative thermal expansion.